Invent. math. 104, 545–580 (1991)

Inventiones mathematicae

The dynamics of complex polynomials and automorphisms of the shift

Paul Blanchard[1], **Robert L. Devaney**[1]*, **and Linda Keen**[2]**

[1] Department of Mathematics, Boston University, Boston, Mass. 02215, USA
[2] Department of Mathematics, Herbert H. Lehman College, CUNY, Bronx, N.Y. 10468

Oblatum 6-XII-1989 & 13-IX-1990

Table of contents

Introduction

The focus of this article is the interplay between two distinct areas of dynamical systems. The first is the study of iteration of polynomials in one complex variable; the second is the study of automorphisms of the one-sided shift.

The most conspicuous feature of a complex polynomial is its *filled-in Julia set*; this is the set of points whose orbits stay bounded under iteration. The filled-in Julia set of a quadratic polynomial is one of two types: it is either connected in which case the unique critical point belongs to the filled-in Julia set, or it is a Cantor set and the critical point escapes to ∞. In higher degrees the situation is more complicated.

We consider the space X_d of monic, centered polynomials of degree d; these are polynomials of the form $z^d + a_{d-2} z^{d-2} + \ldots + a_0$. Every polynomial of degree

* Research supported in part by the National Science Foundation grant #DMS 88-01277
** Research supported in part by the National Science Foundation grants #DMS 870105 and #RII-8903049

d is affine conjugate to one that is monic and centered (by a conjugacy that need not be unique). The *connectedness locus* is the subset of X_d consisting of polynomials whose filled-in Julia set contains all the critical points. The other extreme is the subset, S_d, called the shift locus. This set contains the *shift-like* polynomials; these are polynomials whose filled-in Julia set contains no critical points. In this case the filled-in Julia set is a Cantor set. If $d>2$ there are many polynomials that are in neither the shift locus nor in the connectedness locus. In fact, there are polynomials whose Julia set is a Cantor set but which are *not* shift-like [Br], [B2].

This paper is motivated by what, at first, seems to be a question in combinatorial dynamical systems – the structure of the group automorphisms of the one-sided d-shift. Recall that the sequence space, Σ_d, is the space of semi-infinite sequences with entries from an alphabet of d symbols and that the shift map acts on sequences by dropping the first entry of each sequence. The *automorphism group* Aut_d consists of homeomorphisms of Σ_d that commute with the shift. The groups Aut_d were originally studied by Hedlund [H] in the 1960's; he proved the important result that Aut_2 consists only of the identity and the symbol interchange. More recently, Boyle, Franks, and Kitchens [BFK] showed, by contrast, that when $d>2$, Aut_d is infinitely generated with a rich algebraic structure. Furthermore, Ashley [Ash] exhibited an efficient set of generators called *minimal marker automorphisms.*

Our goal in this paper is to show that there is a surprising relationship between the topology of the shift locus and Aut_d. In particular, we present a geometric method for realizing automorphisms of the d-shift via loops in the shift locus.

The bridge between shift-like polynomials and automorphisms of the shift relies on the following fact: if P is a shift-like polynomial of degree d, its dynamics, when restricted to its Julia set, are conjugate to the one-sided shift on d symbols. Moreover, since the polynomial restricted to the Julia set is hyperbolic, the Julia set varies continuously as we change the polynomial within the shift locus. Thus, a closed loop in the shift locus induces an automorphism of the shift in the natural way: we simply follow points in the corresponding Julia sets as we traverse the loop and the induced map on the Cantor set is an automorphism of the d-shift. We call this automorphism the monodromy induced by the loop. For example, if we look at the monodromy induced by following a loop which winds once around the Mandelbrot set, then we find that the induced automorphism is the unique non-trivial element of Aut_2. In general, we have a representation:

$$\Theta_d\colon \pi_1(S_d) \to \mathrm{Aut}_d.$$

Our main result is:

Theorem *The map Θ_d is a surjection.*

Our methods involve two similar constructions, both of which relate the structure of the dynamical plane to that of the parameter space. The first construction involves "spinning the lowest critical value" around its level curve (in the dynamical plane) of the rate of escape potential. This generates loops in the shift locus which essentially produce the minimal marker automorphisms. The second construction deforms the polynomial through different levels of the potential.

This process produces a tree whose vertices correspond to polynomials to which we apply the spinning construction.

There has been other related work on the realization of automorphisms of the shift. For example, Wagoner [W] has a geometric method for realizing automorphisms of the *two-sided* shifted via monodromies of Axiom A basic sets for diffeomorphisms of high dimensional spheres. Also, there are related results for rational maps in [GK].

The paper is organized as follows. In §1 we discuss the quadratic case and use it to introduce our methods. In §2 we summarize basic results, both from complex analytic dynamics and from symbolic dynamics. The spinning construction is discussed in detail in §3. In §4 we construct the tree which yields the enumeration of the minimal generating set of Aut_3, and we extend this result to the degree d case in §5. In the final section, we briefly describe the relationship between our work and the elegent description of cubic parameter space contained in the two papers of Branner and Hubbard [BH1, BH2].

Acknowledgements. We would like to acknowledge the hospitality of the Mathematics Institute at the Warwick University, the Max-Planck Institut für Mathematik in Bonn, the Institute for Advanced Study in Princeton, and the T.J. Watson Research Laboratories of IBM for partial support while this paper was being written. In addition, we would also like to acknowledge many helpful conversations with J. Ashley, M. Boyle, A. Douady, J. Franks, L. Goldberg, B. Kitchens, J. Milnor, M. Shishikura, D. Sullivan, and especially B. Branner and J. Hubbard.

1 Quadratic maps

1.1 The shift

Let Σ_d denote the space of sequences whose entries are the integers $0, 1, \ldots, d-1$. The space Σ_d is called the (one-sided) sequence space on d symbols. The set Σ_d is a Cantor set with respect to the product topology. In fact, for $s=(s_0\, s_1\, s_2 \ldots)$, $t=(t_0\, t_1\, t_2 \ldots) \in \Sigma_d$, we define the distance

$$d(s,t)=\sum_{i=0}^{\infty} \frac{\delta(s_i, t_i)}{2^i}$$

where δ is the Kronecker delta function. This gives a metric on Σ_d, and this metric induces the product topology (see [D], [Fr], or [W]).

In this metric, two sequences are close provided their first few entries agree. That is, if $s_i=t_i$ for $i=0, \ldots, n$, then it follows that

$$d(s,t) \leqq \frac{1}{2^n}.$$

The (one-sided) shift map on Σ_d (the d-shift) is given by

$$\sigma(s_0\, s_1\, s_2 \ldots)=(s_1\, s_2\, s_3 \ldots),$$

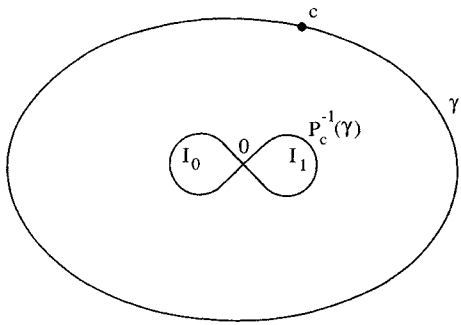

Fig. 1. Construction of I_0 and I_1

i.e., σ simply drops the first entry of each sequence in Σ_d. It is well known that σ is continuous and d-to-1 [D, S]. The shift map is important in a variety of settings, including dynamical systems, probability, coding theory, and information theory.

1.2 The quadratic case

Surprisingly, automorphisms of the 2-shift arise naturally in the study of dynamics of quadratic polynomials. Any quadratic polynomial is affine conjugate to a polynomial of the form $P_c(z)=z^2+c$. The filled-in Julia set of P_c, denoted K_c, consists of the set of points whose orbits are bounded, and the Julia set, J_c, is the frontier of K_c. The Julia set J_c may also be characterized as the closure of the set of repelling periodic points of P_c or as the set of points at which the family of iterates of P_c fails to be a normal family. These definitions were shown to be equivalent, both by Fatou [F] and Julia [J] (see [B] for details).

The polynomial P_c has a unique finite critical point 0 with critical value c. The orbit of 0 plays a crucial role in determining the topological nature of J_c, as illustrated by the following theorem. Although the result is well-known, we include a sketch of the proof of Part B. See [DH2], [B], or [D] for more details.

Theorem 1.1 *Let* $P_c(z)=z^2+c$.

A. *If* $\{P_c^n(0)\}$ *is bounded, then* K_c *and* J_c *are connected.*
B. *If* $P_c^n(0)\to\infty$ *as* $n\to\infty$, *then* J_c *exhausts* K_c *and is a Cantor set which is homeomorphic to* Σ_2. *In this case,* $P_c|J_c$ *is topologically conjugate to the 2-shift.*

Remark. Throughout this paper, for the sake of readability, if γ is a simple closed curve, we will call the interior of the region bounded by γ the *interior of* γ.

A sketch of proof of Part B. It is possible to find a simple closed curve γ that passes through c whose inverse image is a figure eight contained in the interior of γ. Since the critical value lies on γ, $P_c^{-1}(\gamma)$ is a wedge of two simple closed curves meeting at 0. Let I_0 and I_1 denote the interiors of these two curves. See Fig. 1.

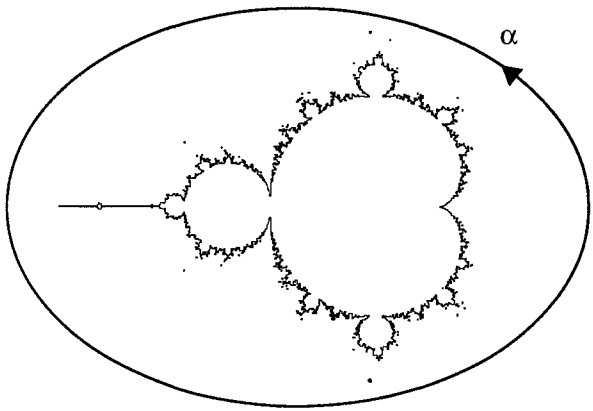

Fig. 2. The loop α in $\mathbf{C}-M$

Since all points in the exterior of $I_0 \cup I_1$ escape under iteration, it follows that $J_c \subset I_0 \cup I_1$.

We now use the itinerary of any point relative to I_0 and I_1 to define the conjugacy to Σ_2. More precisely, if $z \in J_c$, then $P_c^j(z) \in I_0 \cup I_1$ for all j, so we define

$$\ell(z) = (s_0\, s_1\, s_2 \ldots)$$

where $s_j = 0$ iff $P_c^j(z) \in I_0$, $s_j = 1$ iff $P_c^j(z) \in I_1$. Standard arguments [B, D] show that $\ell\colon J_c \to \Sigma_2$ is a homeomorphism. By the definition of ℓ, $\sigma \circ \ell = \ell \circ P_c$. Thus, $P_c | J_c$ is conjugate to the shift. q.e.d.

The following classical result is fundamental to our approach. See [B], [D], or [DH2].

Proposition 1.2 *Suppose $P_c^n(0) \to \infty$ as $n \to \infty$. Then there exists $N > 0$ such that, for all $z \in J_c$ and $n > N$, $|(P_c^n)'(z)| > 1$.*

We remark that a set such as J_c on which $|(P_c^n)'| > 1$ is called a hyperbolic set. Compact hyperbolic sets are important in dynamics because they are structurally stable ([S], [Fr]), which means that they are preserved (up to conjugacy) by perturbations. In particular, in our case, J_c varies continuously with c.

The set of c-values for which K_c is connected is known as the Mandelbrot set. We denote this set by M. It is known that M is a closed, connected set contained in the disk $\{c \mid |c| \leqq 2\}$. See [DH1, Ma].

Consider a closed loop in the c-plane $\alpha\colon [0, 1] \to \mathbf{C} - M$ which winds once around M. See Fig. 2.

For each t, $J_{\alpha(t)}$ is a Cantor set which is conjugate to Σ_2 by Theorem 1.1, and due to the hyperbolicity mentioned in Proposition 1.2, we get a continuously varying one-parameter family of conjugacies

$$\psi_t\colon J_{\alpha(0)} \to J_{\alpha(t)}.$$

Since $\alpha(0)=\alpha(1)$, the map

$$\psi_1 \colon J(P_{\alpha(0)}) \to J(P_{\alpha(0)})$$

is an automorphism of $J(P_{\alpha(0)})$ which commutes with $P_{\alpha(0)}$. We call ψ_1 the **monodromy** associated to α.

We may use the coding map ℓ introduced above to pass from the monodromy ψ_1 of $J(P_{\alpha(0)})$ to an automorphism of Σ_2. We have

$$\begin{array}{ccc} J(P_{\alpha(0)}) & \xrightarrow{\psi_1} & J(P_{\alpha(0)}) \\ \ell \downarrow & & \downarrow \ell \\ \Sigma_2 & \xrightarrow{\theta} & \Sigma_2 \end{array}$$

where $\theta=\ell\circ\psi_1\circ\ell^{-1}$. Hence θ is a homeomorphism.

The map θ commutes with the shift. In particular, note that we have $P_{\alpha(t)}\circ\psi_t=\psi_t\circ P_{\alpha(0)}$ for all t. Therefore,

$$\begin{aligned}\theta\circ\sigma &= \ell\circ\psi_1\circ\ell^{-1}\circ\ell\circ P_{\alpha(0)}\circ\ell^{-1} \\ &= \ell\circ P_{\alpha(0)}\circ\psi_1\circ\ell^{-1} \\ &= \ell\circ P_{\alpha(0)}\circ\ell^{-1}\circ\ell\circ\psi_1\circ\ell^{-1} \\ &= \sigma\circ\theta.\end{aligned}$$

We have now constructed a shift-commuting homeomorphism of Σ_2. Such a map is called an automorphism of the shift.

Automorphisms of the d-shift form a group which we denote by Aut_d. Since Aut_2 consists of just two elements, the identity and the automorphism that interchanges each symbol, it is natural to ask which of these two automorphisms is the map θ.

Theorem 1.3 *Suppose θ is the automorphism of the 2-shift induced by the monodromy associated to a closed curve which winds once around M in $\mathbf{C}-M$. Then θ interchanges 0's and 1's in Σ_2.*

Proof. The automorphism θ is invariant under homotopies in $\mathbf{C}-M$, so it suffices to consider a particular loop in $\mathbf{C}-M$. Let $\alpha(t)=\rho(\cos t+i\sin t)$ where $\rho>2$. Suppose $|z|\geqq\rho$. Then

$$\begin{aligned}|P_{\alpha(t)}(z)| = |z^2+\alpha(t)| &\geqq |z^2|-\rho \\ &\geqq |z|^2-|z| \\ &\quad |z|(\rho-1) \\ &> |z|.\end{aligned}$$

Hence $|P^n_{\alpha(t)}(z)|\to\infty$ if $|z|\geqq\rho$. Therefore we may use the circle $|z|=\rho$ as the curve in the proof of Theorem 1.1 whose preimage defines I_0 and I_1. That is, for each $t\in[0,1]$, let $I_0(t)$ and $I_1(t)$ denote the two components of the interior of the wedge given by

$$P^{-1}_{\alpha(t)}(|z|=\rho).$$

We may choose the indices 0 and 1 so that $I_0(t)$ and $I_1(t)$ vary continuously with t. Indeed, $I_0(t)$ and $I_1(t)$ are given by the two branches of $\sqrt{w-\alpha(t)}$ as w ranges over $|w|<\rho$. Hence, as $\alpha(t)$ traverses the circle of radius ρ, we obtain the maps ψ_t: $J_{\alpha(0)} \to J_{\alpha(t)}$ using the labelling map. Note that the two components $I_0(t)$ and $I_1(t)$ are interchanged when we return to $P_{\alpha(0)}$, that is, $I_0(1)=I_1(0)$ and $I_0(0)=I_1(1)$. It follows that θ interchanges 0 and 1 in the first entry of any sequence, so θ is the non-trivial automorphism of the 2-shift. q.e.d.

Remark. One can see directly that θ interchanges 0's and 1's at the j^{th} entry of any sequence by noting that

$$P^j_{\alpha(1)} \circ \psi_1 = \psi_1 \circ P^j_{\alpha(0)}$$

and then invoking the above argument.

1.3 Spinning the critical value for quadratics

In this section we will give another method to produce the non-trivial automorphism of the 2-shift in complex dynamics. This technique will be the basic operation by which we realize nontrivial automorphisms of the d-shift later. The main tool is the Measurable Riemann Mapping Theorem (MRMT) due to Morrey [Mo] and Ahlfors and Bers [AB]. The idea of using techniques from quasiconformal mappings in dynamics is due to Sullivan [Su].

Throughout this section, we will fix $c=\alpha(0)\notin M$ where $\alpha(t)$ is the loop mentioned in §1.2. Let $D_r=\{z\,|\,|z|\leqq r\}$. Following Douady and Hubbard [DH1], we define the potential, or rate of escape function by

$$h(z)=\lim_{n\to\infty}\frac{\log_+|P_c^n(z)|}{2^n}.$$

The map h is a continuous function on $\mathbf{C}$ (see [DH1] or [BH1] for details). From the definition, we see that

$$h(P_c(z))=2h(z).$$

Define

$$\Gamma_c=\{z\in\bar{\mathbf{C}}\,|\,h(z)>h(0)\}.$$

It is proved in [DH1] that there is a unique analytic homeomorphism

$$\phi_c\colon\ \Gamma_c\to\mathbf{C}-D_R$$

which gives a conjugacy between P_c on Γ_c and $z\mapsto z^2$ on $\mathbf{C}-D_R$ where $R=\exp(h(0))$. If $r>R$, it is known that ϕ_c maps the level curve

$$h(z)=\log(r)$$

to the circle $|z|=r$.

For fixed t, the preimage under ϕ_c of the ray $\rho\mapsto\rho\exp(2\pi it)$, $\rho>R$, is called the external ray of argument t for P_c. We denote this external ray by θ_t. The

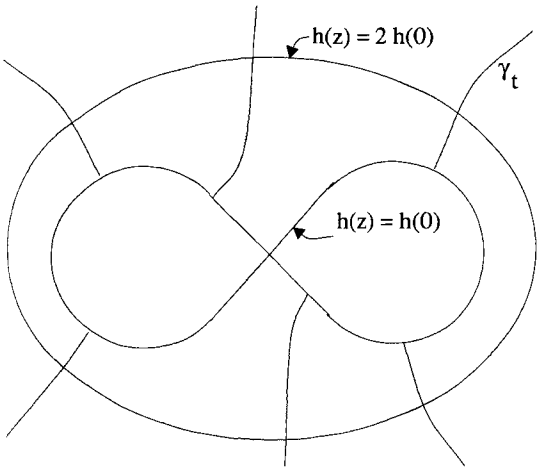

Fig. 3. Polar coordinates on Γ_c

external rays and level sets of the potential h define a system of polar coordinates on Γ_c. See Fig. 3.

The critical value c is in Γ_c and the value $\phi_c(c)$ plays a special role in complex dynamics. In particular, it determines the quadratic polynomial up to affine conjugacy. We call the value $\log|\phi_c(c)|$ the escape rate of the critical value and $\operatorname{Arg}\phi_c(c)$ its external angle.

We now construct a map that we shall later show to be quasiconformally conjugate to P_c. This construction will become the basic procedure by which we deform polynomials in the "spinning construction" below. Choose ρ_1, ρ_2 such that

$$h(c)<\rho_1<\rho_2<2h(c)$$

and consider the annular region

$$A=\{z|\,\rho_1\leqq h(z)\leqq\rho_2\}.$$

Define a Dehn twist τ on A as follows. Let $r_i=e^{\rho_i}$ for $i=1, 2$. Let

$$A'=\{z|\,r_1\leqq|z|\leqq r_2\}.$$

Note that ϕ_c maps A onto A'. Define the usual Dehn twist T on the annulus A' by

$$T(re^{2\pi it})=re^{2\pi i\left(t+\frac{r-r_1}{r_2-r_1}\right)}.$$

Then set

$$\tau(z)=\phi_c^{-1}\circ T\circ\phi_c(z).$$

The map τ is not holomorphic; however, τ is a quasiconformal homeomorphism of A.

Since the annular region A lies between the level sets of the potential containing c and $P_c(c)$, it follows that the inverse image $P_c^{-1}(A)$ is an annular region lying between the level sets of the potential containing 0 and c. Now define

$$F(z)=\begin{cases} P_c(z) & \text{if } z\notin P_c^{-1}(A) \\ \tau\circ P_c(z) & \text{if } z\in P_c^{-1}(A) \end{cases}$$

Clearly, F is a degree two branched cover which differs from P_c only on $P_c^{-1}(A)$. Although F is not a polynomial, the MRMT guarantees that it is quasiconformally conjugate to a polynomial – in fact, to P_c.

Proposition 1.4 *The map F is quasiconformally conjugate to P_c.*

Proof. We define a new conformal structure μ on $\bar{\mathbf{C}}$ which is preserved by F as follows. Let μ_* denote the standard conformal structure on $\bar{\mathbf{C}}$. If $h(z)\geqq h(0)$, we set $\mu(z)=\mu_*(z)$. We then use F to pull back ϕ to $\bar{\mathbf{C}}-J_c$. This defines μ for all $z\in\bar{\mathbf{C}}-J_c$. By construction, F preserves μ. Since μ is the pullback of a complex structure with bounded distortion by a map which is analytic except on $P_c^{-1}(A)$, it follows that μ has bounded distortion on $\bar{\mathbf{C}}-J(P_c)$.

We extend μ to all of $\bar{\mathbf{C}}$ by setting $\mu=\mu_*$ on J_c. We may thus apply the MRMT to obtain a quasiconformal homeomorphism f of $\bar{\mathbf{C}}$ which converts or "straightens" μ to the standard structure μ_* almost everywhere; i.e., $f^*\mu_*=\mu$ a.e. Consequently, the quasiconformal map

$$Q=f\circ F\circ f^{-1}$$

preserves μ_* a.e. and so is analytic on $\bar{\mathbf{C}}$.

We claim that Q is a quadratic polynomial which is affine conjugate to P_c. To see this, we may normalize f so that $f(\infty)=\infty$ and $f(0)=0$. Since f is analytic on a neighborhood of ∞, we may also normalize so that $f'(\infty)=1$. Thus, Q is a degree two map which fixes ∞ and which has branch points at 0 and ∞. Since Q preserves μ_*, Q is analytic. It follows that Q is a polynomial of degree two. Now $F=P_c$ on Γ_c, and f maps the critical orbit of F to that of Q. Hence the external angles and escape rates of the critical values of P_c and Q agree. Therefore, P_c and Q are equal. q.e.d.

Remark. One may, in fact, write down the conjugacy f explicitly. We will actually do this when we apply this construction in the higher degree case. We used the MRMT above since it is essential in the following construction.

We now use the same idea to construct a one-parameter family of maps F_t, $0\leqq t\leqq 1$; we "spin the critical value around a level curve of the potential". We show that each member of this family is quasiconformally conjugate to a polynomial of the form $z^2+c(t)$ where $c(t)$ is continuous and winds once around the Mandelbrot set for $0\leqq t\leqq 1$. Hence this family induces the nontrivial automorphism of Σ_2 as in the previous section.

Define a one-parameter family of annuli A_t for $0\leqq t\leqq 1$ where $A_0=\{z|\,\rho_1\leqq h(z)\leqq\rho_2\}$ as above. For $0\leqq t\leqq 1$, set $\eta_1(t)=(1-\frac{1}{2}t)\,\rho_1$ and $\eta_0(t)=(1-\frac{1}{2}t)\,\rho_2$. Let A_t denote the annular region

$$A_t=\{z|\,\eta_1(t)\leqq h(z)\leqq\eta_0(t)\}.$$

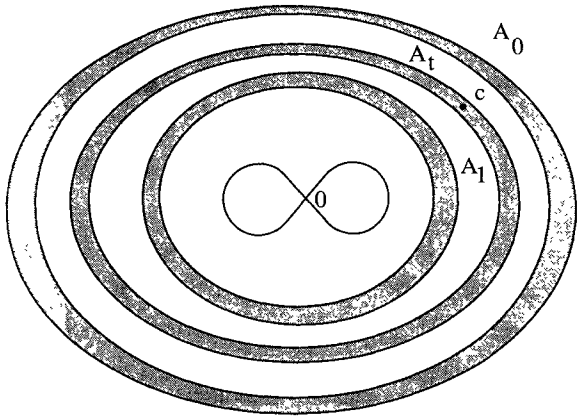

Fig. 4. The annuli A_t

That is, A_t is the annular region whose inner and outer boundary curves are the h-level curves $\eta_1(t)$ and $\eta_0(t)$ respectively. Note that $A_0 = A$ and that A_1 is an annular region contained between the level sets $h(0) = \frac{1}{2}h(c)$ and $h(c)$. See Fig. 4.

For each t we define a Dehn twist τ_t along the level curves of the potential in A_t exactly as we defined τ on A. Then we set

$$F_t(z) = \begin{cases} P_c(z) & \text{if } z \notin P_c^{-1}(A_t) \\ \tau_t \circ P_c(z) & \text{if } z \in P_c^{-1}(A_t) \end{cases}$$

Note that $F_0 = F$. Note also that there is an interval of t-values for which $c = P_c(0) \in A_t$. As t increases, it follows that the critical value $F_t(0) = \tau_t \circ P_c(0)$ is spun once around the level curve $h(z) = h(c)$. When $t = 1$, the critical value returns to its original location, i.e., $F_1(0) = c$.

Proposition 1.5 *The map F_1 is also quasiconformally conjugate to P_c.*

Proof. The proof is the same as before: first define a new F_1-invariant complex structure as in the previous proposition. Use the MRMT with the same normalizations to straighten this structure via a quasiconformal homeomorphism f_1. Then $f_1 \circ F_1 \circ f_1^{-1}$ is a polynomial of degree two. Note that f_1 is analytic on $\{z \mid h(z) > h(0)\}$ and preserves the critical orbit. Hence $f_1 \circ F_1 \circ f_1^{-1}$ is quasiconformally conjugate to P_c as before. q.e.d.

Proposition 1.6 *There is a continuous function $c(t)$, $0 \leqq t \leqq 1$, such that:*

(1) *F_t is quasiconformally conjugate to $z^2 + c(t)$ for each t;*
(2) *$h(c(t))$ is constant; and*
(3) *the external argument of $c(t)$ increases monotonically from 0 to 1 as t increases from 0 to 1.*

Proof. The crucial observation here is that the external rays for P_c are identical to those of F_t in the exterior of $P_c^{-1}(A_t)$. However, the location of the critical value $\tau_t \circ P_c(0)$ relative to these rays changes. Indeed, $\tau_t \circ P_c(0)$ passes through

each ray exactly once as t increases. Thus we may invoke the preceding arguments to show that F_t is quasiconformally conjugate to $z^2+c(t)$ where $c(t)$ satisfies 2 and 3. q.e.d.

Consequently, the polynomials which are conjugate to F_t lie on a loop that winds once around M. As in the previous section, the monodromy map around this loop induces the non-trivial automorphism of Σ_2.

2 The general setting

2.1 Julia sets of higher degree polynomials

Let P be a polynomial of degree d. The Julia set, J_P, is defined exactly as in the quadratic case: J_P is the frontier of the set of points $W^s(\infty)$ whose orbits tend to ∞. If the orbits of all critical points tend to ∞, then the Julia set of P is totally disconnected and $P|J_P$ is topologically conjugate to the d-shift. The proof of this is analogous to the proof of Theorem 1.1; see [B1] for details.

The dichotomy described in Theorem 1.1 for quadratic polynomials no longer holds when $d \geqq 3$. Nevertheless, there is an intimate relationship between the connectivity properties of the Julia set (and filled-in Julia set) and the dynamics of the finite critical points. For example, if all of these orbits are bounded, then $W^s(\infty)$ is simply-connected, and therefore, the Julia set is connected. If at least one critical point iterates to infinity, then the Julia set is disconnected, but it may or may not be totally disconnected.

For example, consider the situation when $d=3$. A generic cubic has two distinct critical points. There are three cases:

(1) Both critical orbits are bounded. Then J_P is connected.
(2) Both critical points are contained in $W^s(\infty)$. Then J_P is a Cantor set, and the dynamics of the polynomial on J_P is hyperbolic and conjugate to the 3-shift.
(3) One critical point iterates to infinity and the other has a bounded orbit. When this happens, the Julia set is disconnected, and it may even be totally disconnected. In addition, there are cubics satisfying these conditions to which one can apply the Douady-Hubbard theory of polynomial-like mappings to show that the Julia set has a countable number of components which are essentially like Julia sets of quadratic polynomials as well as a Cantor set of one-point components [B2]. On the other hand, there are also cubics with one critical point in the Julia set, and every component of the Julia set is a point. However, in these cases, it is interesting to note that, even though the Julia set is totally disconnected, the dynamics is not conjugate to the 3-shift because every sequence has three inverse images under the shift map while the critical value in the Julia set has only two inverse images.

In Chapter 4 we focus on the open subset of parameter space in the second case above.

2.2 Automorphisms of the shift

In this section we recall some of what is known regarding automorphisms of the d-shift σ, particularly when $d \geqq 3$. Recall that $\theta: \Sigma_d \to \Sigma_d$ is an automorphism

of the (one-sided) d-shift if θ is a homeomorphism and $\theta \circ \sigma = \sigma \circ \theta$. Hedlund [H] proved that the only non-trivial automorphism of the 2-shift is the map that interchanges the symbols 0 and 1 independent of their position in the sequence. Similarly, for the d-shift, any permutation of the symbols also yields an automorphism, but there are many automorphisms that do not arise in this manner. In a recent paper, Boyle, Franks, and Kitchens [BFK] studied the group of automorphisms of the d-shift, denoted by Aut_d, $d>2$. This group is infinitely generated and has a rich structure. It is generated by automorphisms that come from permutations of the symbols and by automorphisms of order two which are defined via markers or marker sets [H], [BFK]. More precisely, a marker is a string of symbols of the form $s_0 s_1 \ldots s_k$ together with a pair of symbols α, β. The map generated by this marker simply exchanges α and β whenever α or β is followed by the string $s_0 s_1 \ldots s_k$. For example, the singleton 0 may serve as a marker; the automorphism exchanges 1 and 2 when followed by 0. Thus

$$\theta(102100120\ldots) = (202200110\ldots).$$

It is easy to check that θ is an automorphism of the 3-shift.

A marker set consists of a finite number of strings of symbols together with a pair of symbols to be exchanged. As an example, the pair of symbols 1 and 2 may serve as a marker set for an automorphism of the 3-shift with 1 and 2 exchanged if they are followed by one of these markers, so that the rule is exchange 1 and 2 whenever followed by a non-zero entry. It is convenient to denote this set of markers by $\bar{0}$ (read as "not 0"). This map gives

$$\theta(1012101000\ldots) = (1021101000\ldots)$$

Not all strings of symbols are acceptable markers. For example, the marker 1 preceded by interchange of 1 and 2 is not an automorphism because the map θ is not one-to-one:

$$\theta(111\ldots) = (222\ldots) = \theta(222\ldots).$$

Automorphisms which arise via markers or marker sets are called marker automorphisms.

These results are summarized in the following Theorem from [BFK].

Theorem 2.1 Aut_d *is generated by the union of*

(a) *automorphisms which arise from permutations of the symbols; and*
(b) *a countable set of automorphisms given by markers or marker sets.*

In [BFK], the authors describe a procedure for determining a set of markers or marker sets which generate Aut_d. Ashley [Ash] has refined their results by giving a minimal generating set of marker automorphisms. In the next two sections, we provide a geometric method for realizing this minimal set of generators.

3 The spinning construction

Let X_d be the set of all monic, centered polynomials of degree d. Let S_d denote the subset of X_d consisting of polynomials all of whose critical points escape

to infinity. If $P \in X_d$, there is a neighborhood U of infinity and an analytic homeomorphism ϕ: $U \to \bar{\mathbf{C}} - \bar{D}_r$ such that $\phi \circ P(z) = (\phi(z))^d$. The conjugation ϕ is uniquely determined if we assume that $\phi'(\infty) = 1$. As for quadratics, define the potential function

$$h_P(z) = \lim_{n \to \infty} \frac{\log_+ |P^n(z)|}{d^n}$$

For $z \in U$, let $h_P(z) = \log|\phi(z)|$. Let $c_1, \ldots, c_{d-1}$ be the finite critical points of P and $v_1, v_2, \ldots, v_{d-1}$ be the corresponding critical values. Then S_d can be characterized by

$$S_d = \{P \in X_d \mid h_P(c_i) = \frac{1}{d} h_P(v_i) > 0 \text{ for all } i = 1, \ldots, d-1\}.$$

We will always assume that c_1 is the critical point with the slowest escape rate, i.e., $h_P(c_1) \leqq h_P(c_j)$ for $j = 2, \ldots, d-1$.

Let $P_1, P_2 \in S_d$ and define

$$U_i = \{z \mid h_i(z) \geqq h_i(c_1)\}$$
$$V_i = \{z \mid h_i(z) < h_i(c_1)\}$$

where h_i, c_1 are the corresponding potentials and lowest critical points for P_i. Here, for the sake of readability, we have suppressed the dependence of c_1 on i.

Suppose we have a quasiconformal conjugacy

$$f: U_1 \to U_2$$

between P_1 and P_2. The next two lemmas show that f may be extended to a quasiconformal conjugacy between P_1 and P_2 on all of $\bar{\mathbf{C}}$.

Lemma 3.1 *Let P_i, for $i = 1, 2$, be two polynomials in S_d. If f: $U_1 \to U_2$ is a topological conjugacy, then f can be extended to a conjugacy defined on $\bar{\mathbf{C}} - J_{P_1}$. Moreover, if f: $U_1 \to U_2$ is (K-quasi)conformal, then its extension will also be (K-quasi)conformal.*

Proof. The boundaries of the U_i are level curves of the h_i, and the components of V_i are disjoint, simply-connected domains in $\mathbf{C}$ which we denote D_1^i, $D_2^i, \ldots, D_k^i$. There is a one-to-one correspondence between the boundary curves of U_1 and U_2 given by the map f, and therefore, there is a one-to-one correspondence between these domains. After relabelling, we can assume that f takes the boundary of D_j^1 to the boundary of D_j^2. The conjugacy f is defined inductively over the sets $P_1^{-l}(U_1)$. The inductive step is very similar to the $l = 1$ case, and we present only that case. Suppose that $z \in P_1^{-1}(U_1) \cap D_j^1$. Then, by applying f to $P_1(z)$, we obtain a point w in U_2. There are d inverse images of w under the map P_2 and extending f amounts to determining which of these inverses to pick for $f(z)$. However, we can determine the correct inverse image by noting that exactly one inverse of w is contained in the disk U_j^2. It is this inverse

that is the desired $f(z)$. If f is (K-quasi)conformal, it is clear that, since the P_i are conformal, the extension is also (K-quasi)conformal. q.e.d.

In fact, the conjugacy f above is quasiconformal on all of $\bar{\mathbf{C}}$. The following elegant proof of this fact was shown to us by Douady.

Lemma 3.2 *Suppose P_1 and P_2 are two polynomials in S_d. Let $f: \bar{\mathbf{C}} - J_{P_1} \to \bar{\mathbf{C}} - J_{P_2}$ be a quasiconformal conjugacy. Then f extends to a quasiconformal conjugacy on all of $\mathbf{C}$. In particular, if f is conformal on $\bar{\mathbf{C}} - J_{P_1}$, then P_1 and P_2 are affine-conjugate.*

Proof. Clearly f extends continuously to J_{P_1}, so all we need show is that this extension is quasiconformal. To do this, we will construct a sequence f_n of K-quasiconformal homeomorphisms of $\bar{\mathbf{C}}$ which converge uniformly to f. It then follows that this extension is K-quasiconformal everywhere [A].

Recall that V_1 consists of k disjoint, simply connected regions, $D_1^1, \ldots, D_k^1$. Let us choose any smooth homeomorphism

$$\beta_j: D_j^1 \to \mathbf{C}$$

so that $\beta_j = f$ on the boundary of D_j^1 for each j. We also assume that the β_j are chosen so that

$$f_1(z) = \begin{cases} f(z) & z \in U_1 \\ \beta_j(z) & z \in D_j^1 \end{cases}$$

is a homeomorphism. Since the β_j's are smooth and f is quasiconformal, it follows that f_1 is K-quasiconformal for some K.

We define f_n inductively. Set

$$f_n = P_2^{-1} \circ f_{n-1} \circ P_1$$

where the appropriate branch of the inverse for P_2 is chosen as in the proof of the previous lemma so that f_n is continuous. Note that f_n is K-quasiconformal and that $f_n = f$ on the exterior of kd^n disjoint, simply connected regions in V_1. Since J_{P_i} is hyperbolic, the maximum diameter of any of the images of these regions tends to zero. Therefore, it follows that the f_n converge uniformly to f, and so f is also K-quasiconformal on $\bar{\mathbf{C}}$ q.e.d.

Now we move to the spinning construction. Let $P \in S_d$ and let h be the associated potential. Suppose that $h(c_1) < h(c_j)$ for $j = 2, \ldots, d-1$. Thus there exists $\varepsilon > 0$ such that c_1 is the only critical point in the region $\{z \mid h(z) \leqq h(c_1) + \varepsilon\}$. We also assume that $d^n h(c_1) \neq h(c_j)$ for all $j > 1$ and n. These two assumptions serve to isolate the level sets of the potential corresponding to the orbit of c_1 from all of the other critical levels. Since these level sets are dynamical invariants, this in turn allows us to guarantee the existence of quasiconformal conjugacies during the spinning construction.

Let γ denote the component of $h^{-1}(h(v_1))$ which contains v_1. There are precisely $d-1$ components of $P^{-1}(\gamma)$. We denote them by $\alpha_1, \ldots, \alpha_{d-1}$ and assume that α_1 is the component containing c_1. Hence α_1 is a figure eight,

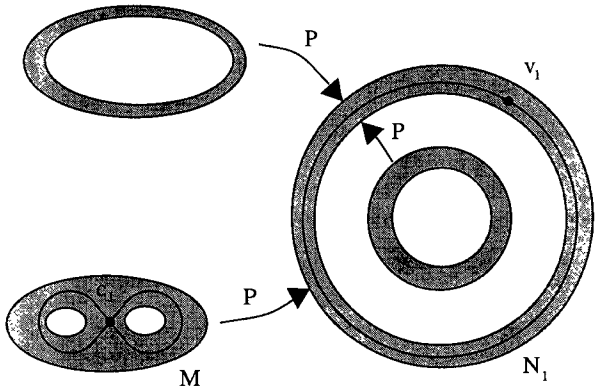

Fig. 5. The components of $P^{-1}(N_1)$, M, N_1

while the remaining α_j are simple closed curves. We may choose $\varepsilon > 0$ small enough so that the region

$$N = \{z | h(v_1) - \varepsilon \leqq h(z) \leqq h(v_1) + \varepsilon\}$$

is disjoint from all of the other critical level curves

$$\left\{z | h(z) = \frac{1}{d^m} h(v_k)\right\}, \quad m = 1, 2, \ldots$$

Let N_1 denote the component of N containing v_1 (and hence γ). It follows that N_1 is an annular region. Let M denote the component of $P^{-1}(N_1)$ that contains c_1. See Fig. 5.

In analogy with the construction in § 1.3, we will modify P on M. For each $t \in [0, 1]$, let A_t be the annular region

$$A_t = \{z \in N_1 | h(v_1) - \varepsilon t \leqq h(z) \leqq h(v_1) + \varepsilon(1-t)\}.$$

Note that A_1 is an annular region bounded by γ on the outside while A_0 is bounded by γ on the inside.

As in § 1.3, there is a conformal map

$$\phi_t \colon A_t \to A_t' = \{\xi | 1 \leqq |\xi| \leqq r_0(t)\}$$

and we may choose ϕ_t so that these maps depend continuously on t. Let

$$T_t \colon A_t' \to A_t'$$

be a Dehn twist, i.e.,

$$T_t(re^{2\pi i s}) = r \exp\left(2\pi i \left(s + \frac{r-1}{r_0 - 1}\right)\right)$$

Let $\tau_t = \phi_t^{-1} \circ T_t \circ \phi_t$. Now define

$$F_t(z) = \begin{cases} P(z) & z \notin M \cap P^{-1}(A_t) \\ \tau_t \circ P(z) & z \in M \cap P^{-1}(A_t). \end{cases}$$

Proposition 3.3 *For all $t \in [0, 1]$, there is a polynomial Q_t such that Q_t is quasiconformally conjugate to F_t.*

Proof. As above, we define a new conformal structure μ_t which is preserved by q_t. Let μ_* be the standard conformal structure. We set $\mu_t = \mu_*$ in the region

$$\{z \mid h(z) > h(v_1) - \varepsilon\}.$$

Let μ_t be the pullback of μ_* by F_t. This defines μ_t everywhere except on J_P. By definition, F_t preserves μ_t.

We define μ_t on J_P by setting $\mu_t = \mu_*$. Since μ_t is given by pulling back a bounded measurable structure by a polynomial, it follows that μ_t is a bounded measurable complex structure as well.

Now apply the MRMT. This gives a quasiconformal homeomorphism f_t which straightens μ_t. We may normalize so that $f_t(\infty) = \infty$. Then we have $f_t \circ q_t \circ f_t^{-1} = Q_t$ is an analytic map of degree d which has a super attracting fixed point at ∞. Therefore, Q_t is a polynomial. If we further normalize so that $f_t'(\infty) = 1$ and $f_t(0) = 0$, then it follows that Q_t is monic and centered.

Proposition 3.4 *In the above construction, both $Q_0 = Q_1 = P$.*

Proof. We will prove this by writing down an explicit conjugacy g_i between F_i and P for $i = 0, 1$. These conjugacies will be quasiconformal. Moreover, they will vanish at 0 and be equal to the identity on a neighborhood of ∞. Hence they are the conjugacies that we obtained by the MRMT in the above argument.

We begin with F_0. Define $\Gamma_r = \{z \mid h(z) > r\}$. Define g_0 to be the identity map on $\Gamma_{h(c_1)+\varepsilon}$. Clearly, we have $g_0 \circ F_0 = P \circ g_0$ on this region.

Let $B \subset M$ be the component of $P^{-1}(A_0)$ which contains c_1. The interior of B is an open annulus. There are two smooth maps $\zeta_i \colon B \to B$, $i = 1, 2$, that satisfy $P \circ \zeta_i = \tau_0 \circ P$. Each of the ζ_i fixes one of the boundary curves of A_0 and rotates the other by a half twist. We choose τ_0 to be the ζ_i which fixes the outer boundary of A_0. Set $g_0 = \tau_0'$ on B. Also define g_0 to be the identity on $\Gamma_{h(c_1)} - B$. It follows that $P \circ g_0 = g_0 \circ F_0$. We now extend g_0 to lower h-levels in the natural way. If z satisfies

$$\frac{1}{d} h(c_1) \leqq h(z) < h(c_1)$$

we set $g_0(z)=P^{-1}\circ g_0\circ F_0(z)$ where we choose the appropriate branch of the inverse of P^{-1} to make g_0 continuous.

It is important to note that $P^{-1}\circ F_0$ is not the identity on the two components of the interior of the figure eight component of α_1. Indeed, g_0 interchanges these two components while preserving the interiors of all other components.

Now continue as in the proof of Lemma 3.1. This defines a quasiconformal homeomorphism of $\mathbf{C}-J_P$ which extends quasiconformally to J_P as in Lemma 3.2. Hence P is quasiconformally conjugate to F_0 via a conjugacy that is the identity on a neighborhood of ∞. Furthermore, g_0 fixes the critical points of P. Hence $P=Q_0$.

We now turn to Q_1. We remark that Q_1 is affine conjugate to P by Lemma 3.3 since f_1 is conformal on $\Gamma_{h(c_1)}$. We prefer, for later purposes, to construct f_1 directly. To do this, define g_1 to be the identity on $\Gamma_{h(c_1)}$. Let B be the component of $P^{-1}(A_1)$ which contains c_1. Note that, unlike the previous case, the interior of B consists of two disjoint annuli each mapped isomorphically onto B by P. We can choose a map τ_1' on each of these components so that $P\circ\tau_1'=\tau_1\circ P$ since P is an isomorphism on each component. Hence we set $g_1=\tau_1'$ on B. Define g_1 to be the identity on $\Gamma_{h(c_1)-\varepsilon}-B$ and then continue as before. It follows again that g_1 is a quasiconformal homeomorphism conjugating P and Q_1. Note that, unlike the previous case, g_1 preserves all components of $\mathbf{C}-\Gamma_{h(c_1)-\varepsilon}$.

Corollary 3.5 *As t decreases from 1 to 0, the components of the interior of $h_{Q_t}^{-1}(h(c_1))$ containing c_1 are interchanged.*

4 The cubic case

In this chapter we show how to generate all automorphisms of the 3-shift via monodromy in the parameter space for cubics.

4.1 Five examples

Before beginning the general construction for cubics, we discuss several illustrative examples. All are contained in the one-parameter family

$$P_a(z)=z^3-3a^2z+5$$

where $a\in\mathbf{R}$. (Note that we are using the form adopted by Branner and Hubbard in their study of cubic polynomials [BH1].) The critical points of P_a are $\pm a$ and the value of the constant term is of little significance other than its being large enough to display all of the desired cases. The five examples that we

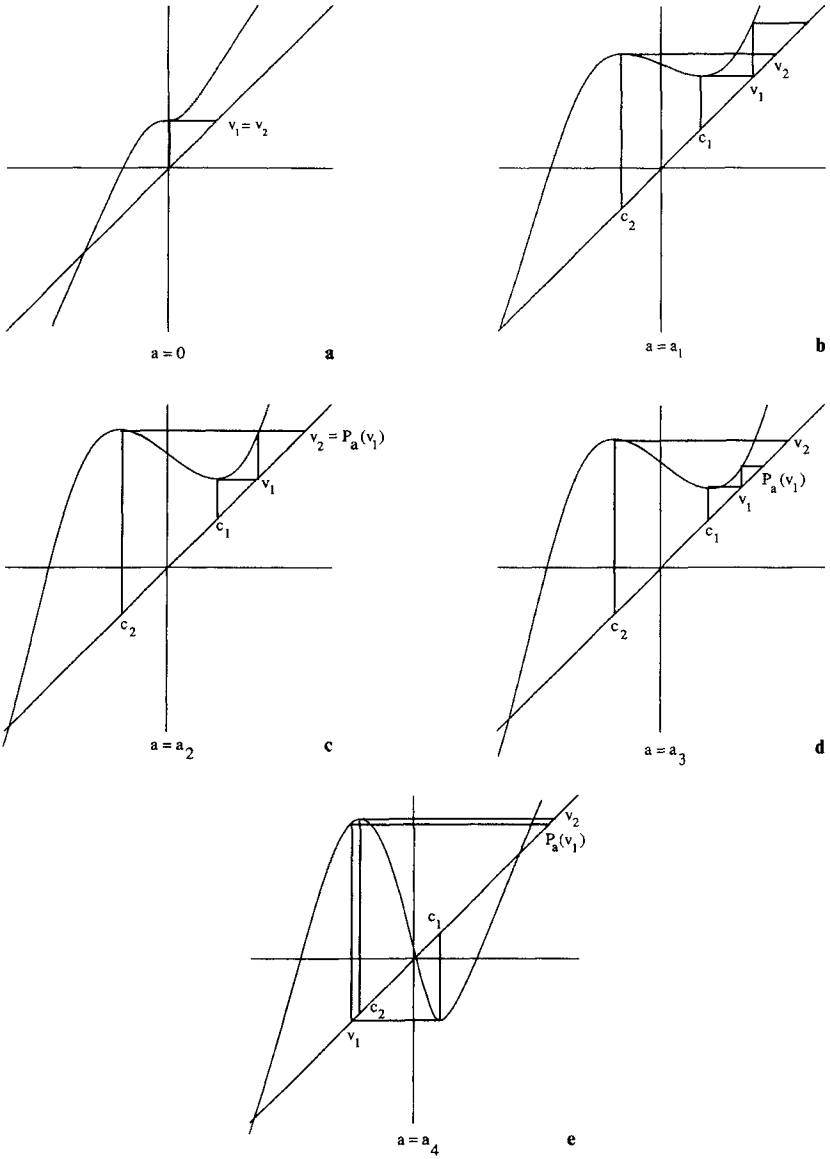

Fig. 6. Graphs of the P_a

discuss are defined by the graphs in Fig. 6. In particular, the a-values are determined by these graphs. Let $h_a(z)$ denote the corresponding potential function.

We show how to generate specific automorphisms of the 3-shift by applying the spinning construction to each of these examples.

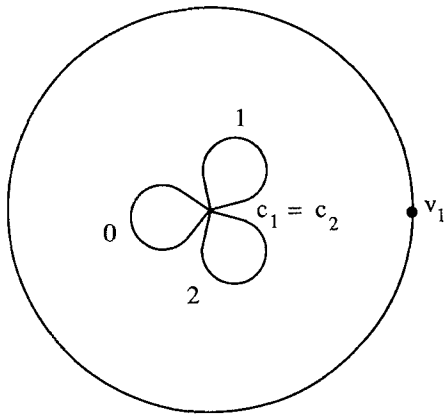

Fig. 7. Level curves for $a=0$

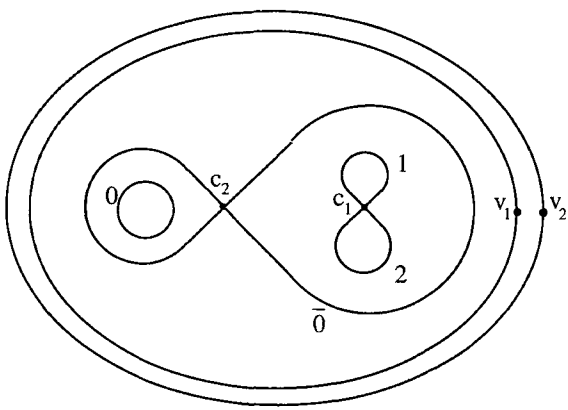

Fig. 8. Level curves for $a=a_1$

Case 1. $a=0$. Certain critical level sets for the potential for $P_0(z)=z^3+5$ are shown in Fig. 7. We denote the 3 components of $h_0(z)<h_0(0)$ by 0, 1 and 2 respectively. Recall that, in the quadratic case, we labelled the analogous components I_0 and I_1 (see the proof of Theorem 1.1). Note that there is an arbitrary choice involved in this selection. If we use the spinning construction of the previous section to spin the critical value around the level set $\gamma=h_0^{-1}(h_0(5))$, then we induce a one-third turn on the lobes of $\alpha=h_0^{-1}(h_0(0))$, and this yields an automorphism that cyclically permutes the symbols.

Case 2. $a=a_1$. According to Fig. 6.

$$h_a(c_1)<h_a(c_2)<h_a(v_1).$$

The critical levels of the potential are shown in Fig. 8. The region $\{z|\, h_a(z)<h_a(c_1)\}$ may still be used to describe the symbolic dynamics. Indeed, the level

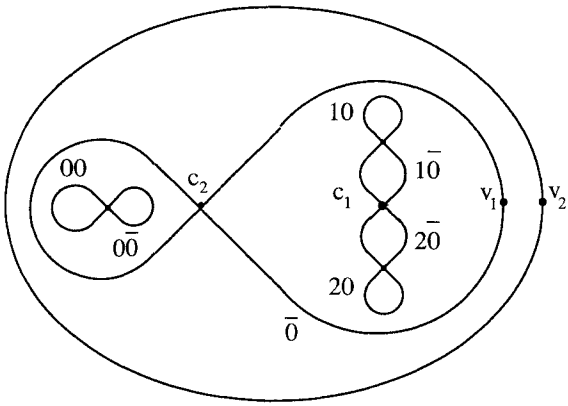

Fig. 9. Level curves for $a=a_2$

curve of $h(z)$ containing c_1 inherits a labelling from Case 1 (see § 4.3). In analogy with §1.2, this labelling indicates the existence of a conjugacy of the Julia set J to Σ_3 where each element of J contained in the disk labelled 0 (or 1 or 2 respectively) is labelled with a sequence starting with the symbol 0 (or 1 or 2 respectively). Note that the lobes numbered 1 and 2 are contained in one component of $\{z|\, h_a(z)<h_a(c_2)\}$, which we call $\bar{0}$ (recall that this is our notation for "not 0"), while lobe 0 is contained within the other component.

If we now spin the critical value v_1 around the curve $\gamma=h_a^{-1}(h_a(v_1))$, the resulting automorphism simply interchanges every 1 and 2; 0 is left fixed.

Case 3. $a=a_2$. This is the special case where $v_2=P_a(v_1)$ and

$$h_a(c_1)<h_a(c_2)=h_a(v_1)<h_a(v_2).$$

The level curves are shown in Fig. 9.

We will not spin the critical value v_1 at this level. However, note how the level sets of $h_a(z)$ pinch. The preimages of c_2 on $h_a^{-1}(h_a(c_1))$ now separate the portion of the Julia set previously marked with s ($s=0, 1, 2$) into two pieces, one marked $s0$, the other marked $s\bar{0}$.

Case 4. $a=a_3$. Now suppose we change the parameter a so that

$$h_a(v_1)<h_a(c_2)<h_a(P_a(v_1))<h_a(v_2).$$

Then the critical level curves of $h_a(z)$ break apart as shown in Fig. 10.

If we now spin the critical value v_1 around its level curve, then only the components of the Julia set marked $1\bar{0}$ and $2\bar{0}$ are interchanged; the components 10 and 20 are left fixed.

Thus, spinning induces the automorphism given by the marker set $\bar{0}$: interchange 1 and 2 whenever followed by 1 or 2.

At this point we note that we have reached the polynomial P_{a_4} by simply "pushing" the critical value v_1 down the real axis. Note that $h_a(v_1)$ decreases during this process. This will be the essential ingredient in the next section when we show how to perform this "pushing deformation" in general.

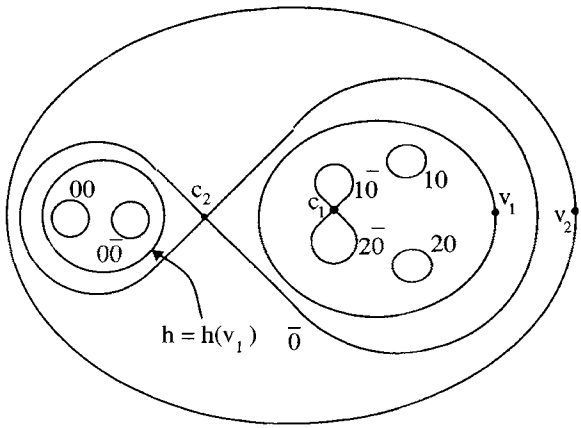

Fig. 10. Level curves for $a = a_3$

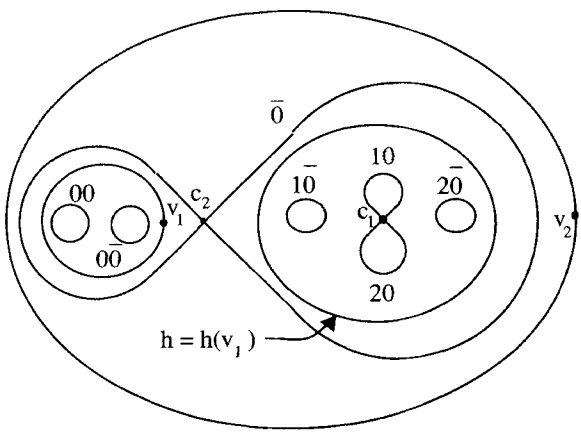

Fig. 11. Level curves for $a = a_4$

Case 5. $a = a_4$. The levels for this a-value satisfy

$$h_a(v_1) < h_a(c_2) < h_a(P_a(v_1)) < h_a(v_2)$$

as before, but note that the critical value v_1 is in the other component of $h(z) = h(v_1)$. The level sets for h_a inherit a different marking in this case. See Fig. 11.

Spinning the critical value here interchanges the components marked 10 and 20, that is, it induces the automorphism with marker 0.

4.2 A tree in the cubic shift-locus

In this section, we construct a tree T in the parameter space for cubics. It is a directed graph with a unique initial vertex. It is connected and has countably many vertices.

The vertices of T correspond to minimal marker automorphisms (see Sect. 2.2). That is, given a minimal marker automorphism θ, there exists a unique vertex P_θ of T such that an application of the spinning construction to P_θ realizes θ. In fact, T will be constructed so that its directed edges correspond to decreasing values of $h(c_1)$. In other words, if $\beta(t)$: $[a, b] \to T$ is a path whose direction agrees with that of T, then

$$\frac{dh(c_1)}{dt} < 0.$$

We define the tree T inductively.

The Initial Vertex ($k=1$):

To start the induction, we use a polynomial whose critical points $\{c_1, c_2\}$ and corresponding critical values $\{v_1, v_2\}$ satisfy the inequalities

$$h(c_2) < h(v_1) < h(v_2).$$

One such polynomial is P_{a_1}, as defined in Fig. 6. The level curves of $h(z)$ for this polynomial are displayed in Fig. 7.

The Inductive Step – The Pushing Deformation:

Each vertex of T at the k-th level corresponds to a polynomial P whose critical points and critical values satisfy the equation

$$h(c_2) < 3^k h(c_1) < h(v_2).$$

Suppose r is a positive real number which satisfies

$$h(v_1) < r < \frac{h(v_2)}{3^{k-1}}.$$

Then the level set $h^{-1}(r)$ consists of a collection of disjoint simple, closed curves $\gamma_1, \ldots, \gamma_m$ and, therefore, the level set $h^{-1}(r/3)$ consists of the curves $\alpha_1, \ldots, \alpha_{3m-1}$. The polynomial P maps all but one of the α_i injectively onto some γ_j, and one α_i (denoted α_1) is mapped onto some γ_j (denoted γ_1) in a two-to-one fashion. Let the Riemann surface S be the component of $h^{-1}([r/3, r])$ which contains v_1. Then γ_1 is one of the boundary curves of S. For example, if we choose r so that

$$h(v_1) < r < h(v_2)$$

for the polynomial P_{a_1} described above, then we obtain the Riemann surface depicted in Fig. 12.

The induction step is based on the following construction (which will be referred to as the pushing deformation below). Given a quasiconformal homeomorphism f: $S \to S$ that restricts to the identity map on ∂S, we will use the MRMT to construct another polynomial P_f. First, we construct an endomorph-

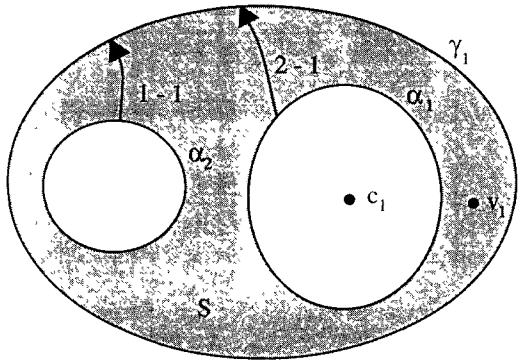

Fig. 12. The Riemann surface S for P_{a_1}

ism F of $\bar{\mathbf{C}}$. Let S' be the component of $P^{-1}(S)$ which contains the critical point c_1. Then define

$$F(z)=\begin{cases} P(z) & z\in\bar{\mathbf{C}}-S' \\ f\circ P(z) & z\in S'. \end{cases}$$

Note that $F(z)$ is conformal outside of S'. Next we define (in the usual manner) an F-invariant quasiconformal structure on $\bar{\mathbf{C}}$ starting with the standard structure on $h^{-1}([r/3, \infty])$. We pull this structure back to $\bar{\mathbf{C}}-J_P$ using F. Finally, we extend the structure to all of $\bar{\mathbf{C}}$ by setting it equal to the standard structure on J_P. This structure has bounded distortion, since F is conformal except on S' and the pullback from S to S' introduces only a finite amount of distortion. By applying the MRMT to this new F-invariant structure, we obtain a quasiconformal homeomorphism f: $\bar{\mathbf{C}}\to\bar{\mathbf{C}}$ such that $f^{-1}\circ F\circ f$ is the desired polynomial P_f.

It is important to note that the above construction is analytic in its parameters (see [AB]). For example, if we apply it to a one-parameter family f_t which varies analytically in t, then the resulting polynomials P_{f_t} also vary analytically in t. In essence, the pushing construction allows us to deform the polynomial using a quasiconformal deformation of the Riemann surface S.

To establish the inductive step, we apply the parameterized version of the pushing construction to the given vertex P of T using special choices of families f_t. Given P, let S be the Riemann surface defined above. Corresponding to any smooth path $\beta(t)$ in S that starts at v_1, we can find a one-parameter family of quasiconformal homeomorphisms f_t: $S\to S$ such that $f_t(v_1)=\beta(t)$. The topology of S determines the number of such paths $\beta(t)$ we use and, therefore, the number of edges of T which leave P.

One component of the level set of level $h(v_2)/3^k$ lies inside S and separates γ_1 from the α-curves on ∂S (see Fig. 13). For each α-curve in ∂S, we construct an edge of T leaving P. In fact, let α_i be one of the α-curves in ∂S. Choose a point v_{α_i} in the component of

$$\{z\,|\,h(z)<h(v_2)/3^k\}\cap(S-\alpha_i)$$

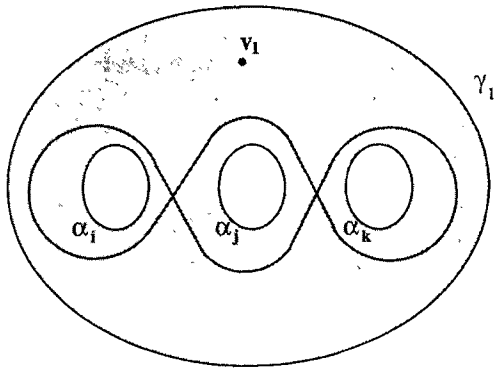

Fig. 13. The twice pinched curve in S is that portion of the level set $h^{-1}(h(v_2)/3^k)$ contained in S

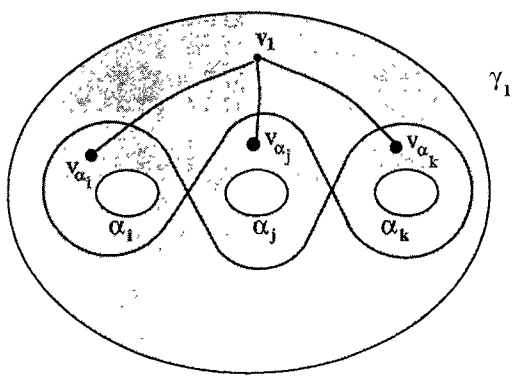

Fig. 14. The inductive step applied to the surface S shown in Fig. 13

bounded by α_i. Connect v_1 to v_{α_i} by a simple curve $\beta(t)$ and apply the pushing deformation with $f_t(v_1)=\beta(t)$. We obtain one edge of T leaving P. The inductive step is complete after we apply the same argument to each α-curve in ∂S (using disjoint paths $\beta(t)$).

When S is a disk minus three holes as in Fig. 14, we obtain three edges leaving P and three new vertices at the $(k+1)$-st level of T (see Fig. 15).

In order to establish the condition

$$\frac{dh(c_1)}{dt} \leqq 0$$

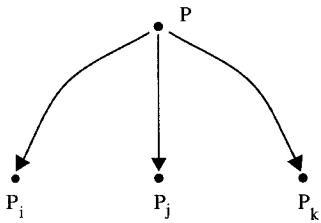

Fig. 15. The branches resulting from Fig. 14

mentioned at the beginning of this section, we need only take care to choose our paths $\beta(t)$ such that

$$\frac{dh_P(\beta(t))}{dt} \leqq 0.$$

Finally, it is important to note that the inductive step is definitely not canonical, and therefore, the resulting tree depends strongly on the choices of the paths $\beta(t)$ used in the construction. This lack of uniqueness is not significant for us, but it causes an ambiguity in the labels introduced in the next section.

4.3 Labelling the level curves of $h(z)$

Now that we have defined the tree in parameter space, we can be more precise about the labelling of level curves of $h(z)$ briefly mentioned in § 4.1. The labels are inherited from a conjugacy of the Julia set to the 3 shift. We first describe this for the initial vertex of T, and then we show how the labelling varies as we move down the tree.

The Initial Vertex ($P = P_{a_1}$ from Fig. 6):

We start by labelling only specific level curves of $h(z)$. Then we extend the labelling scheme to include all level curves whose level is at most $h(c_2)$. Let r be a real number such that

$$h(c_2) < r < h(v_1).$$

Then $h^{-1}(r)$ is a simple, closed curve γ, and $h^{-1}(r/3)$ consists of three simple, closed curves, α_0, α_1, and α_2. Let D_i denote the finite disk bounded by α_i. As in the proof of Theorem 1.1, we define a conjugacy $\phi: J \to \Sigma_3$ by

$$[\phi(z)]_j = i$$

if $P^j(z) \in D_i$. We refer to this process as labelling the curves α_0, α_1, and α_2 with the labels 0, 1, and 2 respectively. In fact, we label the 3^k simple, closed curves in $h^{-1}(r/3^k)$ by the "k-blocks" $(i_0, i_1, \ldots, i_{k-1})$ such that all points $z \in J$ contained inside the curve with label $(i_0, \ldots, i_{k-1})$ satisfy the equation

$$[\phi(z)]_j = i_j \quad \text{for } j = 0, 1, \ldots, k-1.$$

See Fig. 16.

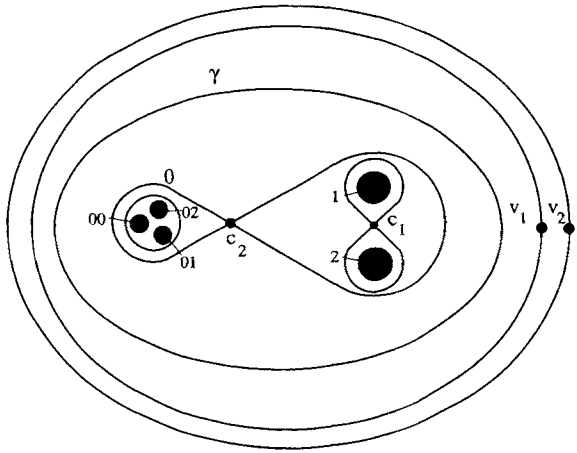

Fig. 16. Preliminary labelling for P_{a_1}

Suppose we assign our initial set of symbols so that blocks beginning with either 1 or 2 are in the same component of $h^{-1}([0, h(c_2)])$ (as in Fig. 16). Then, if we add the additional symbol $\bar{0}$ to our alphabet to represent the union of 1 and 2, we can extend this labelling scheme to all components of all levels $h^{-1}(r)$ when $0<r<h(c_1)$ is a regular value of $h(z)$. Let $\alpha \subset h^{-1}(r)$ be a simple, closed curve. It is labelled by a block of length k where k is determined by

$$\frac{h(c_2)}{3} < 3^{k-1} r < h(c_2)$$

and where the symbols come from $\{0, 1, 2, \bar{0}\}$. Let D_α be the disk in $\mathbf{C}$ bounded by α. The symbols i_j in the block are chosen so that

$$[\phi(z)]_j = i_j \quad \text{for } j=0, \ldots, k-1 \tag{*}$$

for all z in the disk D_α where it is understood that $1=\bar{0}$ and $2=\bar{0}$. Moreover, we only employ the symbol $\bar{0}$ when there is both a $z \in D_\alpha$ with $[\phi(z)]_j = 1$ and another $z \in D_\alpha$ with $[\phi(z)]_j = 2$.

At this point, it is useful to note that we are really labelling the disk D_α as well as the curve α. This makes it easier to see how to label the critical levels of $h(z)$.

Let s be a critical level of $h(z)$. When a component of $h^{-1}(s)$ has l pinch points, we associate $l+1$ distinct labels to that component. If $l=0$, then we follow the procedure for regular levels. However, if $l>0$, then this component bounds $l+1$ disks $D_1, D_2, \ldots D_{l+1}$ in $\mathbf{C}$. We label ∂D_i (disregard the pinch points) with the label assigned to the component of $h^{-1}(s-\varepsilon)$ contained in D_i (where ε is sufficiently small). The points in $J \cap D_i$ satisfy Eq. (*). Again, we emphasize that it is useful to think of the label as a label assigned to the disk D_i as well as to the level curve of $h(z)$.

The results are illustrated in Fig. 17.

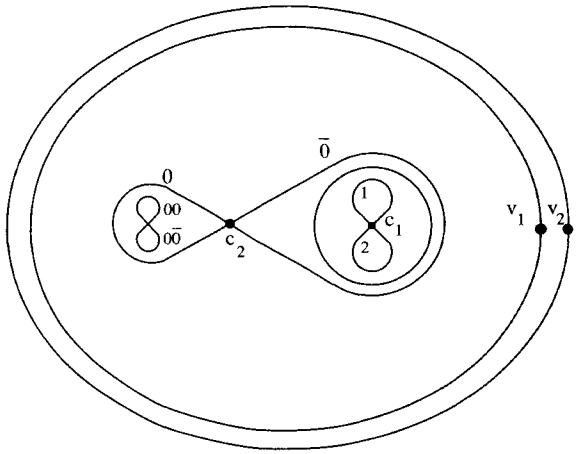

Fig. 17. The complete labelling scheme for P_{a_1}

Labelling all polynomials $P \in T$:

The above labelling scheme can be modified so that we obtain labels for each vertex of T, and these labels specify which automorphism we obtain when apply the spinning construction to the given vertex. Eq. (*) is the key property that we need, and therefore, we must start with a conjugacy to Σ_3. In the construction of the labels for P_{a_1}, we defined a conjugacy ϕ using the level curves of $h(z)$. We are going to use this conjugacy to define all of the other conjugacies we employ. It is important to note that, as we move through the tree, the polynomials are always expanding on their Julia sets. As a result, points in Julia set are not born, nor do they die or coalesce. Given a path Q_t of polynomials in T such that $Q_0 = P_{a_1}$, we extend the conjugacy $\phi\colon J_{Q_0} \to \Sigma_3$ to a one-parameter family of conjugacies $\phi_t\colon J_{Q_t} \to \Sigma_3$ using this hyperbolicity. Once we have fixed the conjugacy ϕ_t, the labelling scheme outlined above extends to Q_t so that Eq. (*) holds. This fact becomes more evident when we indicate below how the labels change as we move along a curve Q_t. It is also useful to note that, once a labelling has been determined for the levels between $h(c_1)$ and $h(c_2)$, it is easy to see how to label the lower levels.

First, we describe the transition in the labelling as we move down from the first to the second level of T. There are two branches of T which leave P_{a_1} corresponding to the fact that the Riemann surface S for P_{a_1} is a disk minus two holes (see Fig. 12), and we indicate how the labels change as we traverse either branch.

Case 1. Let Q_t, where $0 \leqq t \leqq 1$, be the path in T which goes from P_{a_1} to P_{a_3} as indicated in § 4.1. The labelling varies as is indicated in Figs. 8–10, Fig. 18 is an enlargement of the $\bar{0}$ half of the level set through c_2 for Q_1. This example is somewhat misleading because it does not indicate the ambiguity that may arise due to the fact that, in the construction of the tree T, we did not specify a canonical way to choose the curves $\beta(t)$, and therefore, the branches of T are not chosen canonically. In this case, however, we are just following

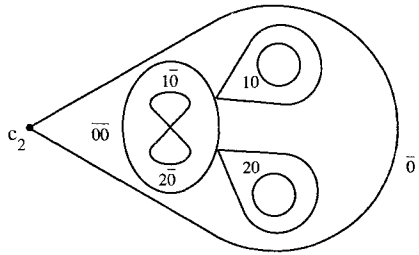

Fig. 18. A more detailed look at some of the levels for P_{a_3}

the parameter a in § 4.1 down the real axis. Therefore, any ambiguity in the labels is hidden by this choice.

Case 2. Let Q_t be the other edge in T which starts at P_{a_1} and ends at a polynomial whose level sets are like those of P_{a_4} in § 4.1. In this case, we cannot avoid the ambiguity mentioned in Case 1 above. The labelling of the pairs $1\overline{0}$, $2\overline{0}$ and 10, 20 depends on the route that Q_t follows as it moves through parameter space. Nevertheless, the figure eight through c_1 is always labelled with the pair 10, 20. It is this pair of labels which indicates which automorphism we obtain when we apply the spinning construction to P_{a_4}.

Now we can describe how the labelling changes in general as we move from a vertex Q_k at the k-th level to a vertex Q_{k+1} at the $k+1$-st level. For Q_k, we have

$$h(c_2) < 3^k h(c_1) < h(v_2).$$

As we move from $Q_k(z)$ to $Q_{k+1}(z)$, the labelling determined by $Q_k(z)$ on

$$h_{Q_k}^{-1}\{(h_{Q_k}(c_1), \infty]\}$$

is inherited by $Q_{k+1}(z)$. Therefore, we need only describe how the labelling changes for the levels between $h_{Q_k}(c_1)$ and $h_{Q_{k+1}}(c_1)$.

In fact, even in this range, most curves inherit the same labels. More precisely, let α be the component of the level curve $h_{Q_k}^{-1}(h_{Q_k}(c_1)+\varepsilon)$ which contains c_1. The labelling only changes for curves within α, and indeed, these changes happen when $h(v_1)$ moves through the value $h(v_2)/3^k$. Parameterize the given edge of T as Q_t where $k \leqq t \leqq k+1$ and suppose that t_0 is the parameter value where $h(v_1) = h(v_2)/3^k$. Then, we need to describe the labelling for three different cases:

Case 1 ($t < t_0$). The labelling is the same as for Q_k. See Fig. 19.

Case 2 ($t = t_0$). In this case, the critical value v_1 lies on a critical level curve of $h(z)$, and the component γ containing v_1 is a pinched curve with m pinch points. Therefore, γ is labelled with $m+1$ k-blocks $B_1, B_2, \ldots, B_{m+1}$. Let B_1 represent the block which corresponds to that part of γ which contains v_1. The component γ' of $Q_{t_0}^{-1}(\gamma)$ containing c_1 has $2m+1$ pinch points. The component is labelled with the $k+1$-blocks $1B_1, \ldots, 1B_{m+1}, 2B_1, \ldots, 2B_{m+1}$, and the two lobes joined at c_1 have the labels $1B_1$ and $2B_1$. See Fig. 20.

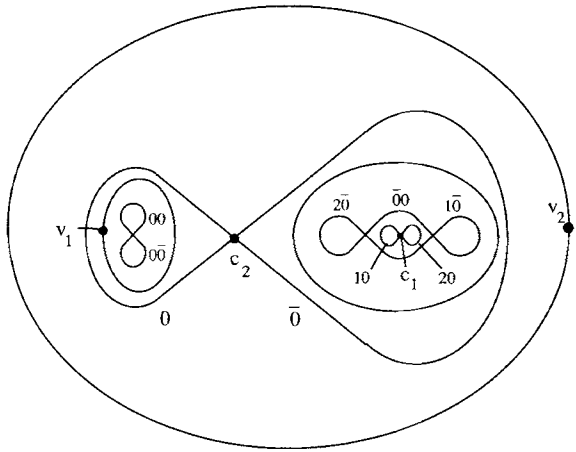

Fig. 19. A typical Q_k

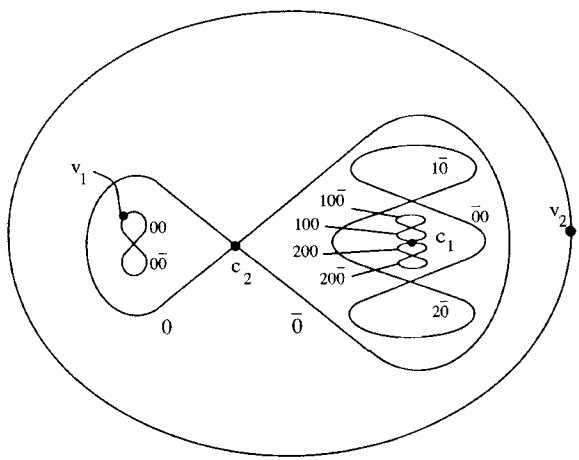

Fig. 20. The labelling for Q_{t_0}

Case 3 ($t > t_0$). The curve γ' in Case 2 is replaced by a critical level which has $2m$ pinch points and the labels $\bar{0}B_1, 1B_2, \ldots, 1B_{m+1}, 2B_2, \ldots, 2B_{m+1}$. The critical point c_1 lies inside the lobe labelled $\bar{0}B_1$ on a figure eight level curve. That level is labelled with the two labels $1B_1$ and $2B_1$. See Fig. 21.

Now given any path Q_t from the initial vertex $Q_0 = P_{a_1}$ of T to a vertex Q_k at the k-th level of T, we can use the above observations to describe a labelling of the level curves of $h_{Q_k}(z)$ which satisfies Eq. (*). In the next section, we prove our main result using this labelling.

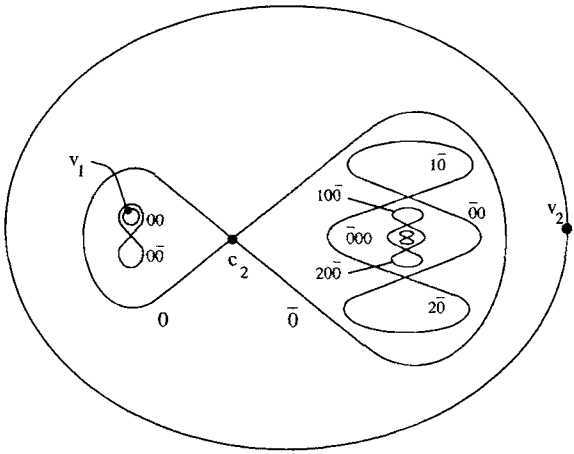

Fig. 21. The labelling for Q_{k+1}

This method of proof above also yields:

Proposition *Let M_j denote the number of vertices of the tree T. Then $M_1=2$ and $M_{j+1}=3M_j-1$.*

4.4 Statement of the main theorem and a table of marker automorphisms

In our construction of trees in the previous section, we showed that, to each vertex of the tree T, there is a loop in the parameter space X_3. This loop was given as follows: start at the polynomial $P_0(z)=z^3+5$; move to the vertex by the pushing deformation; apply the spinning construction; and then return to P_0. If we choose the initial vertex P_0 of the tree as basepoint, we obtain a sequence of based loops, δ_T, in the parameter space. These loops determine a subset of the fundamental group $\pi_1(X_3, P_0)$. We include in δ_T the special loop δ_0 that begins at P_0 and follows the path determined by the spinning the critical value. (Recall case 1, § 4.1)

In [Ash], Ashley defines an algorithm to determine an infinite list of words in the alphabet $\{0, \bar{0}, 1, 2\}$ using *state splitting*. He calls the automorphisms defined by interchanging the symbols 1 and 2 whenever they are followed by one of these words *minimal marker automorphisms*. If a word in the list contains the symbol $\bar{0}$, the corresponding marker set consists of all those markers obtained by replacing $\bar{0}$ with 1's and 2's. He proves that these minimal marker automorphisms together with the automorphism that cyclically permutes the symbols generate Aut_3. He then proves that our algorithm for defining the tree generates the same list.

By our remarks above, any element of $\pi_1(X_3, P_0)$ induces an element of Aut_3 and hence defines a monodromy map Θ_3: $\pi_1(X_3, P_0) \to \mathrm{Aut}_3$. The monodromy map depends on the choice of base point and the labelling homeomorphism l of the Julia set.

Table 1

Length 1:	0	$\bar{0}$				
Length 2:	00	$0\bar{0}$	10	20	$\bar{0}\bar{0}$	
Length 3:	000	$00\bar{0}$	$0\bar{0}0$	$01\bar{0}$	$02\bar{0}$	100
	$10\bar{0}$	200	$20\bar{0}$	110	120	210
	220	$\bar{0}\bar{0}\bar{0}$				
Length 4:	0000	$000\bar{0}$	$00\bar{0}0$	$002\bar{0}$	$001\bar{0}$	0100
	0200	$0\bar{0}0\bar{0}$	$01\bar{0}0$	$011\bar{0}$	$012\bar{0}$	$02\bar{0}0$
	$021\bar{0}$	$022\bar{0}$	1000	$100\bar{0}$	1010	1020
	$10\bar{0}\bar{0}$	2000	$200\bar{0}$	2010	2020	$20\bar{0}\bar{0}$
	1100	$110\bar{0}$	1200	$120\bar{0}$	2100	$21\bar{0}\bar{0}$
	2200	$220\bar{0}$	1110	1210	2110	2210
	1120	2120	1220	2220	$\bar{0}\bar{0}\bar{0}\bar{0}$	

Putting these results together with Ashley's, we obtain:

Main Theorem for cubics *The map Θ_3 is a surjection. Moreover, the set δ_T maps onto a full set of generators of* Aut_3.

Table 1 lists the minimal markers and marker sets of length j for $j=1$, 2, 3, 4. These correspond to the vertices of T at depth j.

5 The higher degree case

We saw in Chapter 3 that the spinning construction works for polynomials of all degrees. Our remarks at the end of Chapter 4 also generalize so that there is a well defined monodromy map Θ_d: $\pi_1(X_d, P_0) \to \mathrm{Aut}_d$. As above, this map depends on a choice of basepoint and labelling homeomorphism. Below, using arguments analogous to those for the cubic case, we define a tree T^d, and use it to construct based loops in $\pi_1(X_d, P_0)$. These loops, together with a special one obtained by spinning the critical value of $P_0(z)=z^d+5$ form a set δ_{T^d}. We will prove:

Theorem 5.1 *The monodromy map Θ_d is a surjection. Moreover, the set δ_{T^d} maps onto a full set of generators of* Aut_d.

As we saw for quadratics and cubics, the polynomial $P_0(z)=z^d+5$ plays a special role in our theory: the arguments of Chapter 3 and the examples in Chapter 4 generalize to show that spinning the unique critical value $v=5$ about the level curve $\gamma=h^{-1}(h(5))$ induces a $1/d$ rotation on the d lobes of the level curve $\alpha=h^{-1}(h(0))$. This in turn realizes the automorphism that cyclically permutes the symbols.

Recall that the minimal marker automorphisms of Aut_3 consist of a infinite list of words in the alphabet $\{0, \bar{0}, 1, 2\}$ where the automorphism is defined by interchanging the symbols 1 and 2 whenever they are followed by one of these words. If the word contains the symbol $\bar{0}$ the corresponding marker set consists of all those markers obtained by replacing $\bar{0}$ with 1's and 2's. Each word in this list corresponds to a vertex of the tree T^3.

In degree d, we begin with the alphabet $\{\bar{0}, 0, 1, 2, 3, 4, \ldots, d-1\}$, where following Ashley's notation, $\bar{0}$ stands for 1 or 2 and does not stand for *not*

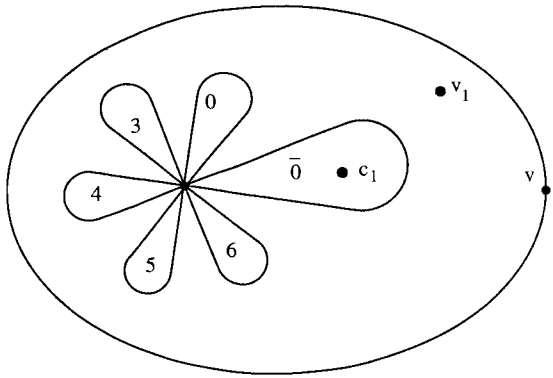

Fig. 22. Level curves of P_0

0. We define a tree T^d for polynomials of degree d whose vertices correspond to words in this alphabet. Ashley's state splitting algorithm for $d>3$ differs only in the initialization and again gives an infinite list of words that determine the minimal generating set of marker automorphisms. In any degree, our algorithm for defining the tree will yield the same list as Ashley's algorithm.

We choose as initial point of the tree a polynomial P_0 whose level curves have the following properties. See Fig. 22

(1) All critical points $c_j, j=2, \ldots, d-1$ are equal.

(2) The critical points are labelled so that their escape rates are in increasing order; that is, c_1 has a slower escape rate than c_2.

(3) The critical levels satisfy the inequalitites:

$$h_{P_0}(c_2)<h_{P_0}(v_1)<h_{P_0}(v_2)$$

We now use essentially the same inductive procedure we developed in §4.2 to complete the tree so that the relative h-levels of v_1 vary with respect to those of v_2.

That is, at the first step, we use the *pushing deformation* on P_0, to push the critical value down into any one of the $d-1$ lobes of the curve $\alpha=h^{-1}(h(0))$. Spinning the critical value about its resulting level curve determines the first level of the tree. The vertices are labelled $\{\bar{0}, 0, 3, 4, \ldots, d-1\}$. See Fig. 22.

The argument at the k-th level is almost a verbatim copy of the inductive step in § 4.2; the only changes are to replace every occurrence of the number 3 with the number d and to replace the alphabet for the labelling scheme so that it is $\{\bar{0}, 0, 1, 2, \ldots, d-1\}$.

The proof that Ashley's minimal marker automorphisms are in one-to-one correspondence with the vertices of the tree is exactly as in the cubic case. It follows that, by spinning the lowest critical value of the polynomials of degree d, $d\geqq 3$, we obtain all the minimal marker automorphisms. Since we also obtain the automorphism that cyclically permutes the symbols we conclude that the monodromy map Θ_d is a surjection. This completes the proof of Theorem 5.1. We remark that the above construction does not yield all of the generators of π_1, since we have assumed that $v_1=v_2\ldots=v_{d-1}$.

6 Topology of the Branner-Hubbard locus

In [BH1, BH2] Branner and Hubbard describe in detail the parameter space of cubic polynomials. We summarize some of their results below and relate them to our work.

We defined our parameter space X_3 as the space of monic, centered polynomials, that is, polynomials of the form $z^3+\alpha z+\beta$. Branner and Hubbard use a slightly different space of polynomials. They consider polynomials of the form

$$P_{a,b}(z)=z^3-3a^2z+b; \quad (a,b)\in\mathbf{C}^2$$

where a and b are complex parameters. Note that $P_{a,b}$ has critical points at $\pm a$. Let P_3 denote the space of all such polynomials.

Define the potential function $h_P(z)$ as before to measure the rate at which points escape to ∞. Also let $\phi(z)$ be the uniformizing function that conjugates the polynomial $P(z)$ to z^3 in a neighborhood of ∞.

The *connectedness locus* in parameter space is the set of polynomials neither of whose critical points escapes to infinity; that is, the set

$$\{P_{a,b}|h(a)=h(-a)=0\}.$$

Branner and Hubbard [BH1] prove that the connectedness locus is compact and cell-like.

We come next to the complement of the connectedness locus. Let c_2 be the critical point that escapes faster and set

$$\mathscr{S}_r=\{P_{a,b}|h(c_2)=\log r\}$$

for $r>1$. It is proved in [BH1] that $\mathscr{S}_r$ is homeomorphic to a sphere of dimension 3. The sphere $\mathscr{S}_r$ may be decomposed into two subsets $\mathscr{S}_r^{\pm}$, depending on whether $c_2=\pm a$. The interiors of $\mathscr{S}_r^{\pm}$ are solid tori unknotted in $\mathscr{S}_r$. They are linked in $\mathscr{S}_r$ with linking number 3. These tori may be further decomposed into slices $Y_r^{\pm}(t)$ where

$$\phi(P(c_2))=r^3\exp(2\pi it).$$

Each slice consists of a trefoil clover leaf. The common boundary point of the three closed disks composing the clover leaf is a polynomial of the form $P(z)=z^3+b$. Each disk is determined by the choice of a cube root of $\exp(2\pi it)$. The argument t defines the external ray for the polynomial.

Since the shift locus S_3 is contained in the complement of the connectedness locus, its topology is determined from the Van Kampen theorem by the decomposition above and a discussion of the topology of $Y_r^{\pm}(t)\cap S_3$ for fixed r and t [BH2].

Fix r and t and let L be the portion of $Y_r^{\pm}(t)\cap S_3$ which is contained in one of the three leaves in a slice. Thus the complement of L consists of polynomials for which the orbit of c_1 is bounded. It is known that the components

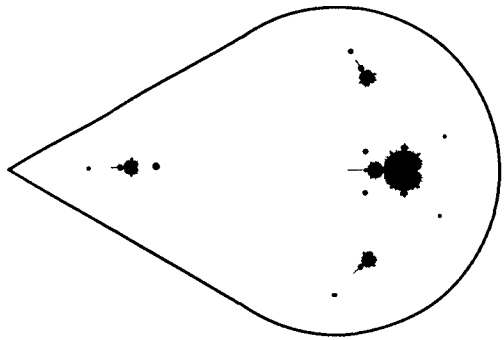

Fig. 23. Points and Mandelbrot sets in L

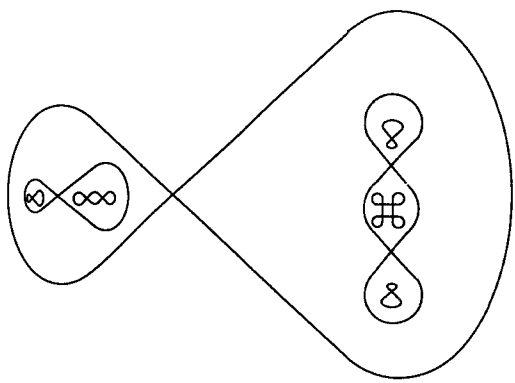

Fig. 24. Critical level curves in L

of the complement of L fall into two infinite subsets: points and homeomorphic copies of the Mandelbrot set. See Fig. 23.

L may be decomposed into open subsets by removing the *critical level curves*. These curves consist of polynomials for which $3^k h(c_1)=h(c_2)$ for some $k\in\mathbf{Z}$. See Fig. 24. See also Fig. 10.1 in [BH2]. Let $\tilde{L}$ denote L with critical level curves removed. Branner and Hubbard have shown that $\tilde{L}$ is a countable union of annuli. Moreover, any two polynomials inside a given component of $\tilde{L}$ are quasiconformally conjugate.

We now relate our results to this picture. Recall that we produced automorphisms via two operations in parameter space, the spinning construction and the pushing deformation. In any loop generated in parameter space by spinning, all of the polynomials are quasiconformally conjugate. It follows that this loop lies entirely inside one of the components of $\tilde{L}$. When the resulting automorphism is non-trivial, the loop in this component is not contractible in the annulus. This means that we may label each annulus in $\tilde{L}$ by the unique

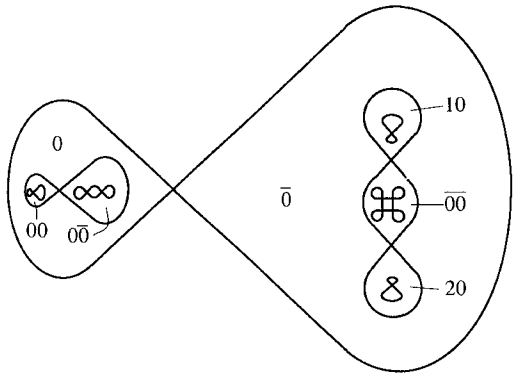

Fig. 25. Automorphisms and the Branner-Hubbard locus

minimal marker automorphism given by spinning around this loop. On the other hand, the pushing deformation allows us to pass through critical level curves and descend through the various components of $\tilde{L}$. The tree generated by these deformations thus tell us how the annuli fit together in the Branner-Hubbard locus, and our main theorem for cubics says that all such components may be identified in this manner. In Fig. 25 we have displayed the various minimal marker automorphisms corresponding to annuli in $\tilde{L}$.

References

[A] Ahlfors, L.: Lectures on Quasiconformal Mappings. Princeton, N.J. Van Nostrand, 1966

[AB] Ahlfors, L., Bers, L.: The Riemann Mappings Theorem for Variable Metrics. Ann. Math., II. Ser. **72**-2, 385–404 (1960)

[Ash] Ashley, J.: Marker Automorphisms of the One-Sided Shift. Ergodic Theory Dyn. Syst. **10**, 247–262 (1990)

[BFK] Boyle, M., Franks, J., Kitchens, B.: Automorphisms of the One-Sided Shift and Subshifts of Finite Type. Ergodic Theory Dyn. Syst. **10**, 421–449 (1990)

[B1] Blanchard, P.: Complex Analytic Dynamics on the Riemann Sphere. Bull. Am. Math. Soc., New Ser. **11**, No. 1, 85–141 (1984)

[B2] Blanchard, P.: Disconnected Julia Sets. In: Chaotic Dynamics and Fractals, Ed. M. Barnsley, S. Demko, Academic Press, (1986), pp. 181–201

[BH1] Branner, B., Hubbard, J.: The Iteration of Cubic Polynomials I: The Global Topology of Parameter Space. Acta Math. **160**, 143–206 (1988)

[BH2] Branner, B., Hubbard, J.: The Iteration of Cubic Polynomials II. Patterns and Parapatterns. Acta Math (to appear)

[Br] Brolin, H.: Invariant Sets under Iteration of Rational Functions. Ark. Mat. **6**, 103–144 (1965)

[D] Devaney, R.L.: An Introduction to Chaotic Dynamical Systems, second edition. Redwood City, Calif.: Addison-Wesley Co. 1987

[DH1] Douady, A., Hubbard, J.: Itération des Polynômes quadratiques complexes. C.R. Acad. Sci., Paris, Ser. I, **29**, 123–126 (1982)

[DH2] Douady, A., Hubbard, J.: Étude Dynamique des Polynôme Complexes. Publ. Math. Orsay. 84–102 (1984)

[DH3] Douady, A., Hubbard, J.: On the Dynamics of Polynomial-like Mappings. Ann. Sci.

Ec. Norm. Super., IV. Ser. **18**, 287 (1985)
[F] Fatou, P.: Sur les Equations Fonctionelles, Bull. Soc. Math. Fr. **47**, 161–271 (1919)
[Fr] Franks, J.: Homology and Dynamical Systems. Conf. Board Math. Sci. Regional Conference Series. **49** (1982)
[GK] Goldberg, L., Keen, L.: The Mapping Class Group of a Generic Quadratic Rational Map and Automorphisms of the Two Shift. Invent. Math. **101**, 335–372 (1990)
[H] Hedlund, G.: Endomorphisms and Automorphisms of the Shift Dynamical System. Math. Syst. Theory **3**, 320–375 (1969)
[J] Julia, G.: Iteration des Applications Fonctionelles, J. Math. Pures Appl., 47–245 (1918)
[LV] Lehto, O., Virtannen, K.I.: Quasi Conformal Mappings. Berlin Heidelberg New York: Springer 1965
[Ma] Mandelbrot, B.: The Fractal Geometry of Nature. San Francisco: Freeman and Co. 1982
[Mi] Milnor, J.: Remarks on Iterated Cubic Maps, SUNY Stony Brook 1990/6
[Mo] Morrey, C.B.: On the Solutions of Quasi-Linear Elliptic Partial Differential Equations. Trans. Am. Math. Soc. **43**, 126–166 (1938)
[S] Smale, S.: Diffeomorphisms with Many Periodic Points. In: Differential and Combinatorial Topology. (pp. 63–80) Princeton: Princeton University Press 1965
[Su] Sullivan, D.: Quasiconformal Maps and Dynamical Systems I, Solutions of the Fatou-Julia Problem on Wandering Domains. Ann. Math., II. Ser. **122**, 401–418 (1985)
[W] Wagoner, J.: Realizing Symmetries of a Shift. Ergodic Theory Dyn. Syst. **8**, 459–481 (1988)